

KANQAS: Kolmogorov-Arnold Network for Quantum Architecture Search

Akash Kundu^{*,a}, Aritra Sarkar^{†,b}, Abhishek Sadhu^{‡,c}

^{*} QTF Centre of Excellence, Department of Physics, University of Helsinki, Finland

^{*} Institute of Theoretical and Applied Informatics, Polish Academy of Sciences, Gliwice, Poland

^{*} Joint Doctoral School, Silesian University of Technology, Gliwice, Poland

[†] QuTech, Delft University of Technology, Delft, The Netherlands

[‡] Raman Research Institute, Bengaluru, India

[‡] Centre for Quantum Science and Technology (CQST), International Institute of Information Technology, Hyderabad, Telangana, India

^aCorresponding Author: akash.kundu@helsinki.fi

^b: a.sarkar-3@tudelft.nl

^c: abhisheks@rri.res.in

Abstract—Quantum architecture search (QAS) is a promising direction for optimization and automated design of quantum circuits towards quantum advantage. Recent techniques in QAS focus on machine learning-based approaches from reinforcement learning, like deep Q-network. While multi-layer perceptron-based deep Q-networks have been applied for QAS, their interpretability remains challenging due to the high number of parameters. In this work, we evaluate the practicality of Kolmogorov-Arnold Networks (KANs) in QAS problems, analyzing their efficiency in the task of quantum state preparation and quantum chemistry. In quantum state preparation, our results show that in a noiseless scenario, the probability of success and the number of optimal quantum circuit configurations to generate the multi-qubit maximally entangled states are $2\times$ to $5\times$ higher than Multi-Layer perceptions (MLPs). Moreover, in noisy scenarios, KAN can achieve a better fidelity in approximating maximally entangled state than MLPs, where the performance of the MLP significantly depends on the choice of activation function. In tackling quantum chemistry problems, we enhance the recently proposed QAS algorithm by integrating Curriculum Reinforcement Learning (CRL) with a KAN structure instead of the traditional MLP. This modification allows us to design a parameterized quantum circuit that contains fewer 2-qubit gates and has a shallower depth, thereby improving the efficiency of finding the ground state of a chemical Hamiltonian. Further investigation reveals that KAN requires a significantly smaller number of learnable parameters compared to MLPs; however, the average time of executing each episode for KAN is higher.

I. INTRODUCTION

Recent research has advanced quantum computing concepts and software development, yet significant challenges remain before real-world applications are feasible. Automating quantum algorithm design via Machine Learning (ML) and optimization algorithms offers promising solutions to enhance quantum hardware and programming capabilities for complex problems. Strongly inspired by Neural Architecture Search (NAS) [1], Quantum Architecture Search (QAS) [2], [3] is introduced.

QAS encompasses techniques to automate the optimization of quantum circuits and it typically consists of two parts. In the first part, a template of the circuits is built where the circuit can

have parameterized quantum gates, e.g., rotation angles. Then, these parameters are determined via the variational principle using a classical optimizer in a feedback loop. Algorithms constructed via this technique are called Variational Quantum Algorithms (VQA) [4], [5]. The parameterized circuit design in VQAs is critical, as it directly influences the expressivity and efficiency of the quantum solution. Recently, QAS has been utilized to automate the search for optimal parameterized circuits for VQAs. QAS also finds application in determining non-parameterized circuits as an approach for quantum program synthesis [6] and multi-qubit maximally entangled state preparation [7].

One of the most prominent methods to tackle QAS problems is to use Reinforcement Learning (RL) (RLQAS) [8], [7], [9], [10], [11], [12]. In this approach, quantum circuits are defined as a sequence of actions generated by a trainable policy. The cost function's value, optimized independently by a classical optimizer, serves as a signal for the reward function. This reward function guides the policy updates to maximize expected returns and select optimal actions for subsequent steps. Maximization of the expected return is achieved by training neural networks (NNs). Recently, NNs have shown potential in quantum information tasks [13], [14]. RLQAS with deep NNs can overcome the trainability issues of VQAs [15], [16] and has demonstrated promising outcomes in NISQ hardware [10], [11].

In a recent work [17], researchers have introduced Kolmogorov-Arnold Networks (KANs) as a novel neural network architecture typically poised to replace traditional Multi-Layer Perceptrons (MLPs). Contrary to the universal approximation theorem-based MLPs, KAN utilizes the Kolmogorov-Arnold representation theorem to approximate complicated functions. KAN has linear weights replaced by spline-based univariate functions along the network edges and is structured as learnable activation functions. Such a design enhances the accuracy and interpretability of the networks, enabling them to achieve comparable or superior results with smaller network sizes across a range of tasks, including data fitting

and solving partial differential equations. Recently, different variants of KAN have been introduced [18], [19], [20], [21], [22], [23]. KAN has applications in time series analysis [24], [25], [26], satellite image classification [27], and improving the robustness of neural network architectures [28]. To understand the full potential and limitations of KANs there is a need for further investigation towards robustness and compatibility with other deep learning architectures.

In this article, we evaluate the practicality of KANs in quantum circuit construction, analyzing their efficiency in terms of the probability of success, frequency of optimal solutions and their dependencies on various degrees of freedom of the network. To the best of our knowledge, the application

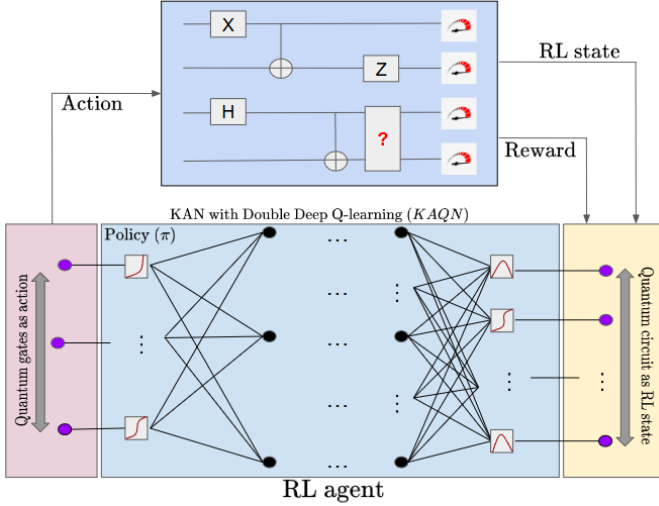


Fig. 1: The schematic for KANQAS shows how the Kolmogorov Arnold network replaces the multi-layer perceptron structure in the RL agent. The environment, which is the quantum circuit, interacts with the RL agent (containing the KAN) and gets updates after each step after the agent decides on an action following a policy.

of Kolmogorov-Arnold Networks in Quantum Architecture Search is still lacking in standard literature. We propose the application of KAN in QAS by replacing the MLP of Double Deep Q-Network (DDQN) in RLQAS with KAN to generate the desired quantum state, introducing KANQAS¹. As shown in Figure 1, the proposed framework of KANQAS features an RL agent, which contains the KAN, interacting with a quantum simulator. The agent sequentially generates output actions, which are candidates for quantum gates on the circuit. The fidelity of the state from the constructed circuit is compared to the quantum state fidelity of the circuit and is evaluated to determine how far it is from the desired goal. The reward, based on fidelity, is sent back to the RL agent. This process is repeated iteratively to train the RL agent. We show that in a noiseless scenario when constructing Bell and GHZ states, the probability of success and the number of optimal quantum circuit configurations to generate the states are significantly higher than MLPs. In a noisy scenario, we show that KAN can achieve a better fidelity in approximating GHZ state than MLPs, where the performance of the MLP significantly depends on the depth of the network and choice of activation

¹Link to KANQAS code repository

function. We also address quantum chemistry problems, where we find the ground state of 4-qubit H_2 and LiH molecules using recently proposed Curriculum Reinforcement Learning for Quantum Architecture Search (CRLQAS) [11]. In our version of CRLQAS, we replace the MLP structure with KAN in the curriculum reinforcement learning subroutine. Our results show that KAN demonstrates the ability to provide a more compact parameterized quantum circuit, in terms of less number of 2 qubit gates and depth for finding the ground state of the chemical Hamiltonian using VQE, with a significantly reduced number of learnable parameters.

The structure of the paper is as follows. We present the problem statement in Sec. II. In Sec. III, we provide the methods used in this work. Specifically, we introduce the Kolmogorov-Arnold Q Network in Sec. III-A and discuss the RL state, action and reward function in Sec. III-B. We present our results in Sec. IV. Specifically, we discuss the results of our noiseless simulations in Sec. IV-A1, noisy simulations in Sec. IV-A2 and the resource requirements for the simulations in Sec. V. We provide concluding remarks and discuss open problems in Sec. VI.

II. PROBLEM STATEMENT

A. Quantum state preparation

To evaluate the efficiency of RL-assisted KANQAS in quantum circuit construction we check if, in a noiseless and noisy scenario, multi-qubit entanglement can be generated as expected. To this end, we target the generation of two kinds of quantum states: Bell and Greenberger-Horne-Zeilinger (GHZ) states. A Bell state is a maximal 2-qubit entangled state and is given by

$$|\Phi^+\rangle = \frac{1}{\sqrt{2}} (|00\rangle + |11\rangle). \quad (1)$$

The optimal circuit to produce a Bell state is given by

$$\quad (2)$$

Meanwhile, a GHZ state is a 3-qubit maximally entangled state given by

$$|GHZ\rangle = \frac{1}{\sqrt{2}} (|000\rangle + |111\rangle) \quad (3)$$

and the optimal circuit produces a GHZ state given by

$$\quad (4)$$

As a measure of the efficiency of the network, we define the probability of success and the probability of optimal success. The probability of success is given by

$$\frac{\text{Number of times the network finds an admissible circuit}}{\text{Total number of admissible circuits}}, \quad (5)$$

As the problem statement clarifies, any circuit that generates a Bell state and a GHZ state is considered an admissible circuit. Meanwhile, Figure 2 and 4 are optimal admissible circuits to generate 2- and 3-qubit maximally entangled state.

B. Quantum chemistry

Quantum chemistry [29] utilizes quantum mechanics to understand the behavior of atoms and molecules. Its main goal is to understand the electronic structure of chemical systems and dynamics, enabling predictions about their chemical and physical properties. This involves examining electronic ground and excited states, reaction pathways, and transition states, which are crucial for explaining reactivity and interactions within chemical systems.

The Variational Quantum Eigensolver (VQE) is a quantum-classical algorithm that is designed to find the ground state energy of quantum systems, making it particularly useful for studying molecular systems where traditional computational methods may struggle due to the complexity and the exponentially growing size of the systems.

In VQE, the objective is to find the ground state energy of a chemical Hamiltonian H by minimizing the energy

$$C(\vec{\theta}) = \min_{\vec{\theta}} \left(\langle \psi(\vec{\theta}) | H | \psi(\vec{\theta}) \rangle \right). \quad (6)$$

The trial state $|\psi(\vec{\theta})\rangle$ is prepared by applying a Parameterized Quantum Circuit (PQC), $U(\vec{\theta})$, to the initial state $|\psi_{\text{initial}}\rangle$, where $\vec{\theta}$ specify the rotation angles of the local unitary operators in the circuit.

The structure of the PQC is one of the crucial factors affecting the performance of the VQE. Among the recently proposed RLQAS methods for automating the search for PQC in VQE, Curriculum Reinforcement Learning (CRL) for QAS, i.e., CRLQAS [11] demonstrates promising outcomes to find the ground state of various chemical Hamiltonian in the noiseless scenario and under hardware error with short PQCs.

Hence, to evaluate the efficiency of KAN in PQC construction for quantum chemistry problems we replace the MLP structure utilized in CRLQAS with KAN. Utilizing the CRL-assisted KANQAS we find the ground state of 4-qubit H_2 and LiH molecules. The exact molecular structures of these molecules are provided in Table I.

III. METHODS

A. Kolmogorov-Arnold Q Networks (KAQN)

In a recent work [17], Kolmogorov-Arnold Networks (KAN) was proposed as a promising alternative to the Multi-Layer Perceptrons (MLP). KAN is based on the Kolmogorov-Arnold representation theorem [30] instead of the Universal Approximation Theorem [31] used in MLP. The Kolmogorov-Arnold representation theorem states that a real-valued, smooth and continuous multivariate function $g(\mathbf{t}) : [0, 1]^n \rightarrow \mathbb{R}$ can be represented by a superposition of univariate functions [30]

$$g(\mathbf{t}) = \sum_{j=1}^{2n+1} \Psi_j \left(\sum_{k=1}^n \psi_{jk} \right), \quad (7)$$

where $\Psi_j : \mathbb{R} \rightarrow \mathbb{R}$ and $\psi_{ij} : [0, 1] \rightarrow \mathbb{R}$. In other words, any multivariate continuous function on a bounded domain can be expressed as a composition of continuous functions of one variable. This reduces the task of learning complex multi-variable functions to learning a polynomial number of single-variable functions. It was noted by the authors of [17] that the representation of the function in Eq. (7) has two layers of nonlinearity with $2n + 1$ terms in the middle layer, and we need to find functions Ψ_i and ψ_{ij} to approximate $g(\mathbf{t})$. The function ψ_{ij} may be approximated using B-splines [32].

A spline is a piecewise smooth polynomial function defined by a set of control points. It is defined by the order l of the polynomial used to interpolate the curve between the control points. We denote the number of segments between adjacent control points as G . The data points are connected by the segments to form a smooth curve having $G + 1$ grid points. It is observed that Eq. (7) can be represented as a two-layer network having activation functions at the edges and nodes performing the summation operation. However, such a network is too restrictive to approximate any arbitrary function. A way to overcome this was proposed in [17], where the authors propose a general architecture with wider and deeper KANs.

The authors of [17] define a KAN layer by a matrix Ψ of trainable univariate spline functions $\{\psi_{jk}(\cdot)\}$ with $j = 1, \dots, n_i$ and $k = 1, \dots, n_o$, where n_i and n_o denotes the number of inputs and outputs respectively. The Kolmogorov-Arnold representation theorem can be expressed as a two-layer KAN. The inner functions constitute a KAN layer with $n_i = n$, $n_o = 2n + 1$ while the outer function is another KAN with $n_i = 2n + 1$, $n_o = n$. We define the shape of a KAN by $[n_1, \dots, n_k]$ with k denoting the number of layers of the KAN. The Kolmogorov-Arnold representation theorem can be expressed as a KAN of shape $[n, 2n + 1, 1]$. A deeper KAN can be expressed by the composition k layers:

$$\mathbf{z} = \text{KAN}(\mathbf{t}) = (\Psi_k \circ \Psi_{k-1} \circ \dots \circ \Psi_1)\mathbf{t}. \quad (8)$$

Since all functions are differentiable, KAN can be trained using backpropagation [33]. For the sake of simplicity, we describe a 2-depth KAN as $[n_i, n, n_o]$, where the input layer is not included in the depth count. The output and input layers will be comprised of n_o , and n_i nodes corresponding to the total amount of time steps while n describes the number of the hidden layers.

KAN can learn features and compositional structure due to their outer structure resembling MLPs and optimize the learned features by approximating the univariate functions with high accuracy due to their internal spline structure. It should be noted that increasing the number of layers of the dimension of the grid increases the number of parameters and, hence, the complexity of the network.

Motivated by the developments in [34], we replace the Multi-Layer Perceptron (MLP) component of Deep Q-Networks (DQN) with the KAN. Furthermore, we employ the Double Deep Q-Network (DDQN) update rule to enhance stability and learning efficiency. DDQN [35] is a Q-learning algorithm based on standard DQN [36], which features two neural networks to increase the stability of the prediction of

Molecule	Basis	Fermion to qubit mapping	Geometry	Number of qubits
H ₂	sto3g	Jordan-Wigner	H (0, 0, -0.35); H (0, 0, 0.35)	4
LiH	sto3g	Parity	Li (0, 0, 0); H (0, 0, 3.4)	4

TABLE I: List of molecules included in our simulations, with configuration coordinates provided in angstroms.

Q-values for each state and action pair. For more details, see Appendix A.

Throughout the paper, the configurations of KANs and MLPs are written using the short notation: KAN_{d,N_l} for a KAN and MLP_{d,N_l} for an MLP. Here, d is the depth (excluding the input layer) of the network, and N_l is the number of neurons per hidden layer. For example, a KAN with the structure $[n_i, 3, 3, 3, n_o]$ is written as $\text{KAN}_{4,3}$, where the depth d is 4 and each hidden layer has $N_l = 3$ neurons.

B. RL state, action space and reward function

The RL environment in KANQAS is encoded using the tensor-based one-hot encoding method described in [11]. However, the tensor’s dimensions vary depending on the size of the action space. The RL state encoding translates a quantum circuit into a tensor of size $D \times N \times (N + N_{\text{rot}})$, where D is a hyperparameter and is defined as the maximum depth of the circuit, N is the number of qubits and N_{rot} defines the number of 1-qubit gates. The first $N \times N$ encodes the position of the 2-qubit gate and the remaining $N \times N_{\text{rot}}$ encodes the position of the 1-qubit gate. Meanwhile, the definition of the reward function varies depending on the problem under consideration. These aspects are further elaborated in the following sections

a) Quantum state preparation: In this problem, we initialize with an empty quantum circuit (i.e. without any gates). Depending on a fidelity-based reward function of the form

$$R = \begin{cases} \mathcal{R}, & \text{if } F(s_t) \geq 0.98 \\ F(s_t), & \text{otherwise} \end{cases} \quad (9)$$

and by following an ϵ -greedy policy the RL agent sets the probability of selecting a random action. Where $F(s_t)$ is the fidelity of a state at step t generated by KANQAS and $\mathcal{R} \gg F(s_t)$, is a hyperparameter.

The random action is chosen from a predefined action space (\mathbb{A}) which contains non-parametrized 1- and 2-qubit gates [7]

$$\mathbb{A} = \{CX, X, Y, Z, H, T\}. \quad (10)$$

Depending on the action the RL state, which is encoded into a tensor of dimension $D \times N \times (N + 5)$, is modified in the next step.

b) Quantum chemistry: Following the same principle as discussed in the previous section, in this problem, we initialize with an empty quantum circuit (i.e. without any gates). However, for a fair comparison with MLP bases CRLQAS, we utilize a reward function of the form

$$R = \begin{cases} 5 & \text{if } C_t < \xi, \\ -5 & \text{if } t \geq T_s^e \text{ and } C_t \geq \xi, \\ \max\left(\frac{C_{t-1}-C_t}{C_{t-1}-C_{\min}}, -1\right) & \text{otherwise} \end{cases} \quad (11)$$

where C_t is the VQE cost function (see Eq. 6) at RL step t and ξ , is a hyperparameter, but for VQE it is the chemical accuracy 0.0016 Hartree. The random action is chosen from a predefined action space (\mathbb{A}) which contains parametrized 1- and non-parameterized 2-qubit gates [11], [9], [8]

$$\mathbb{A} = \{CX, RX, RY, RZ\}. \quad (12)$$

Depending on the action the RL state, which is encoded into a tensor of dimension $D \times N \times (N + 3)$, is modified in the next step.

IV. RESULTS

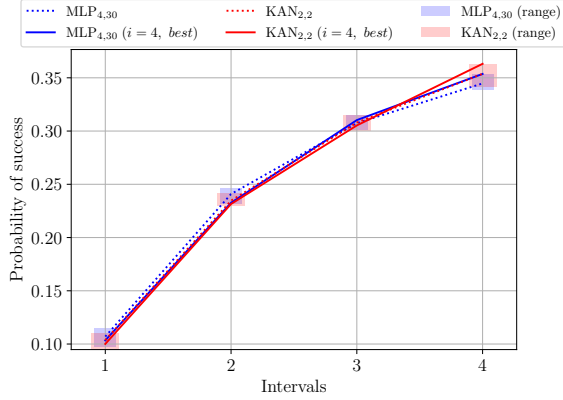
A. Quantum state preparation

1) Noiseless simulation: In the noiseless case, we consider the structure of the KAN and the MLP as presented in Table V. In the case of MLP, the activation function is a hyperparameter and is fixed throughout the training, but in KAN, it is learnable. For the construction of Bell state, we run a total of 10000 episodes where each episode is divided into 6 steps. For a better intuition, we divide the total number of episodes into 4 intervals where each interval contains 2500 episodes.

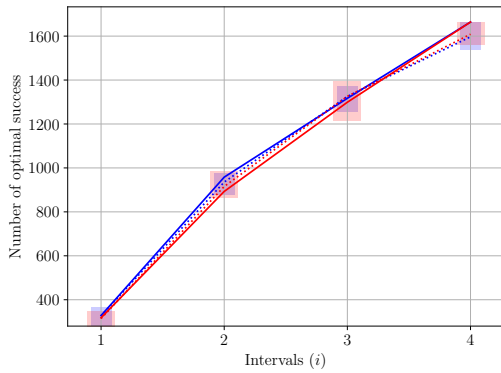
In Figure 2(a) investigate the probability of success in each interval which is calculated as per Eq. 5. Meanwhile, in Figure 2(b), we see the variation in the number of the optimal admissible circuits in each interval. In each interval, the probability is averaged over 20 random seeds, where each seed corresponds to the random initialization of the network. The probability of success with an MLP and KAN is comparable in the first 3 intervals, but in the 4th interval, i.e., in the episodes, falls in the range of 7500 – 10000, the probability of success achieved by KAN is higher. With MLP, the best probability of success achievable in the 4th interval is 35.36% whereas with KAN, we can achieve a success probability 36.31% but the number of optimal admissible ansatz achievable by both the networks is the same. This indicates that KANs have the potential to generate more diverse solutions to the same problem than MLPs.

Meanwhile, the difference in performance between KAN and MLP becomes significant in the task of constructing the GHZ state. Here we consider a depth 2 MLP with 3 neurons ($\text{MLP}_{2,3}$) and depth 4 MLP with 30 neurons ($\text{MLP}_{4,30}$) and compare its performance with a depth 2 KAN containing 3 neurons ($\text{KAN}_{2,3}$). We run a total of 8000 episodes where each episode is divided into 12 steps. Just like the previous 2-qubit experiment, we divide the total number of episodes into 4 intervals where each interval contains 2000 episodes.

In Figure 3(a) we observe that the average probability of success with ($\text{KAN}_{2,3}$) is higher than both $\text{MLP}_{2,3}$ and $\text{MLP}_{4,30}$ over 15 random initialization of the networks. This difference becomes truly significant when we consider the best performance at the 4th interval. *With $\text{KAN}_{2,3}$ we can achieve*



(a)



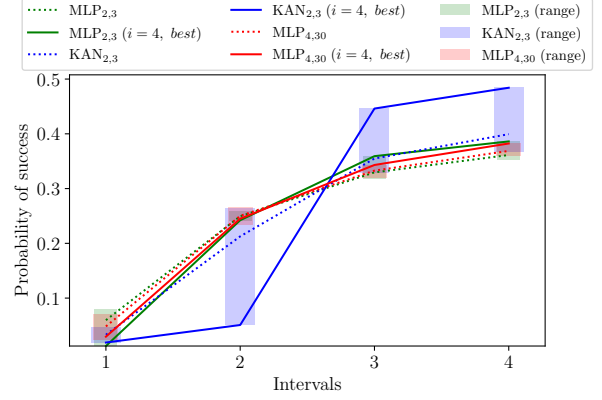
(b)

Fig. 2: In (a) the probability of successful circuits and in (b) the probability of optimal successful circuits in finding a 2-qubit maximally entangled state is slightly higher with KAN than MLP. A total of 10000 episodes are divided into 4 separate intervals where each interval contains 2500 episodes. In (a), each point in an interval corresponds to the probability of occurrence of a successful episode (see Eq. 5). Similarly, (b) corresponds to the number of occurrences of an optimal successful episode. The results are averaged over 20 random seeds (i.e. initialization) of the networks.

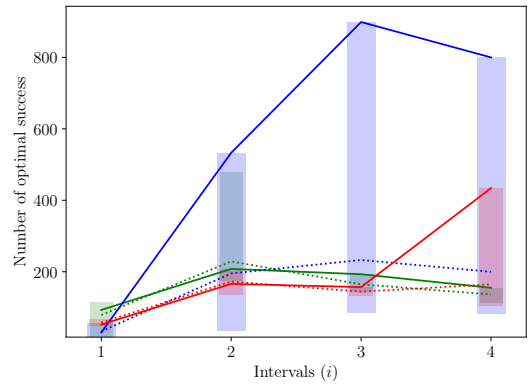
a probability of success in the final interval 48.41% whereas with $MLP_{2,3}$ and $MLP_{4,30}$ we get 38.23% and 38.61% respectively, indicating a 10.18 – 9.8% performance enhancement with KAN.

In Figure 3(b) we observe that on average (over 15 random initialization of the networks) one can achieve a higher number of optimal admissible ansatz using $KAN_{2,3}$ than the MLPs. Meanwhile, when we consider the best performance in the 4th interval the number of optimal admissible ansatz achievable by KAN is 1.84× to 5.16× higher than $MLP_{2,3}$ and $MLP_{4,30}$ respectively.

2) *Noisy simulation*: For the noisy simulation of Bell state preparation, we consider two forms of gate errors depending on the number of qubits. The gate error refers to the imperfection in any quantum operation we perform. For the 1-qubit gate error, we consider random X noise where with probability p_x an X gate is applied to the circuit and with $1 - p_x$ it applies an \mathbb{I} . Meanwhile, for 2-qubit gate error, we apply depolarizing



(a)



(b)

Fig. 3: In (a) the probability of successful circuits and in (b) the total number of optimal successful circuits in finding a 3-qubit maximally entangled state is noticeably higher with KAN than MLP. A total of 8000 episodes are divided into 4 separate intervals, where each interval contains 2000 episodes. In (a), each point in an interval corresponds to the probability of occurrence of a successful episode (see Eq. 5). The results are averaged over 15 random seeds (i.e. initialization) of the networks. The *range* defines the best performance of each interval for both networks. The *range* defines the region between the best and the worst performance in each interval for both networks.

noise which replaces the state of any qubit with a random state of probability p_{dep} . The configuration of MLP and KAN utilized are summarized in Table IV-A2.

At the first stage, we consider noise levels $p_x = 0.1$ and $p_{dep} = 0.01$, where the $MLP_{4,30}$ (i.e. an MLP of depth 4 and 30 neurons) we can achieve a fidelity 99.25% whereas the same fidelity can be achieved with KAN with just depth 2 and 2 neurons.

To elevate the hardness of the problem, in the second experiment, we consider the following noise levels: $p_x = 0.3$ and $p_{dep} = 0.2$. With KAN configuration presented in Table IV-A2 we can achieve a fidelity of 73.28% which $MLP_{4,30}$ with ReLU and LeakyReLU activation functions cannot achieve. Even when the number of neurons is increased tenfold com-

Network	Configuration	Spline and grid	Activation func.	Fidelity
KAN _{3,10}	[84, 10, 10, 12]	B-spline, $k = 4, G = 5$	learnable	0.7328
MLP _{4,30}	[84, 30, 30, 30, 12]	NA	ReLU	0.5005
		NA	LeakyReLU	0.7300
MLP _{4,100}	[84, 100, 100, 100, 12]	NA	ELU	0.6830
			ReLU	0.7300
			LeakyReLU	0.8500

TABLE II: KAN outperforms most of the configurations of MLPs except when MLP_{4,100} is operated with LeakyReLU activation function for noisy Bell state preparation with $p_x = 0.3$ and $p_{\text{dep}} = 0.2$. This helps us conclude that to achieve competitive/better performance with an MLP, it is necessary to fine-tune not just the network’s depth and width but also the activation function.

pared to KAN, MLP_{4,100} (i.e., MLP with depth 4 and 100 neurons) still fails to surpass KAN’s fidelity using ELU and ReLU activation functions. However, with LeakyReLU activation, it achieves a higher fidelity of 85%.

Hence, to achieve competitive/better performance with an MLP, it is necessary to fine-tune not just the network’s depth and width but also the activation function. However, with KAN, this process becomes much simpler, as the activation functions are learnable.

One can argue that KAN has two additional parameters: splines (k) and grid (G) and tuning these hyperparameters can heavily affect the performance of the KAN. In Fig. 5, for constructing GHZ state, we show that to achieve better performance in terms of the depth and number of gates variation in the number of splines (i.e. k) is more effective and stable for the network than variation in G . Whence, in ref. [26], the authors show that achieving a better minimization of the loss function grid size within the splines of KANs has a notable impact. Meanwhile, loss function minimization is crucial for Variational Quantum Algorithms (VQAs), so it is much needed to fine-tune the grid size while optimizing parameterized gates within parameterized quantum circuits of VQAs.

B. Quantum chemistry

In this section, we utilize the recently introduced CRLQAS [11] algorithm to automate the search for a parameterized quantum circuit to find the ground state of 4-qubit H₂ and LiH in the noiseless scenario. Replacing the MLP in the curriculum reinforcement learning algorithm in CRLQAS by KAN, we evaluate the performance of the neural networks. The molecular structure of the H₂ and LiH are discussed in detail in Appendix B in Tab. I.

In finding the ground state of H₂ molecule, we consider an MLP of depth 6, containing 1000 neurons i.e. MLP_{6,1000}, which is compared with a KAN of depth 4 with 3 neurons i.e. MLP_{4,3}. Meanwhile, to find the ground state of LiH molecule we consider MLP_{4,100} and compare its performance with KAN_{4,3}. For more details on the configuration of the neural networks see Tab. VI.

In Fig. 4, we benchmark using the total number of 2-qubit gates, the circuit depth, and the total number of gates in the parameterized quantum circuit. These parameters are labeled as 2-qubit gate, Depth, and Numb. gate on the x-axis of Fig. 4. In both cases, we observe that KAN_{4,3} outperforms various MLP configurations in terms of average (minimum)

depth and 2-qubit gate count. This indicates that KAN_{4,3} can find more compact parameterized quantum circuits for solving the H₂ and LiH molecules compared to MLP_{6,1000} and MLP_{4,100}. However, the total number of gates required to solve these problems is smaller with MLP, suggesting that for a parameterized quantum circuit with fewer 1-qubit gates, it is preferable to choose MLP over KAN in CRLQAS.

In Appendix C, we further investigate two different configurations of KAN and MLP to find the ground state of the 4-qubit LiH. The results reveal that while larger configurations, such as MLP_{6,1000}, outperform KAN, they require 5-100× more learnable parameters. However, when considering a comparable number of learnable parameters, for instance, MLP_{4,500} and KAN_{4,50}, KAN achieves the ground state with a parameterized quantum circuit of smaller depth and fewer 2-qubit gates. Although MLP results in a lower error in estimating the ground state, our objective in quantum chemistry is to attain chemical accuracy, defined as 1.6×10^{-3} Hartree² [37]. Given that the noise in 2-qubit gates is significantly higher than in 1-qubit gates [38], KAN demonstrates considerable promise for solving quantum chemistry problems on real quantum hardware.

V. RESOURCE DETAILS

Here we quantify the resources required by KAN and MLP for the simulations presented in the previous section. In this quantification, we consider (1) the total number of learnable parameters and (2) the time of execution of each episode with the two networks.

A. Parameter count

With depth L and width N MLP only needs $O(N^2L)$ parameters whereas KAN requires $O(N^2L(G+k))$ parameters. In Table III for the quantum state generation problem and in Tab. VII for quantum chemistry problems, we calculate the total number of learnable parameters required for KANs and MLPs in noisy and noiseless scenarios. We observe that in all cases KAN requires a lesser number of parameters than MLP.

B. Time of executing each episode

Although KAN requires fewer learnable parameters than MLPs, the average time of executing each episode for KAN

²The chemical accuracy is often defined as being within 1 kcal/mol, which is an experimental value, as 1 Hartree = 627.5095 kcal/mol, therefore 1 kcal/mol is equal to approximately $0.0015934 \approx 0.0016$ Hartree

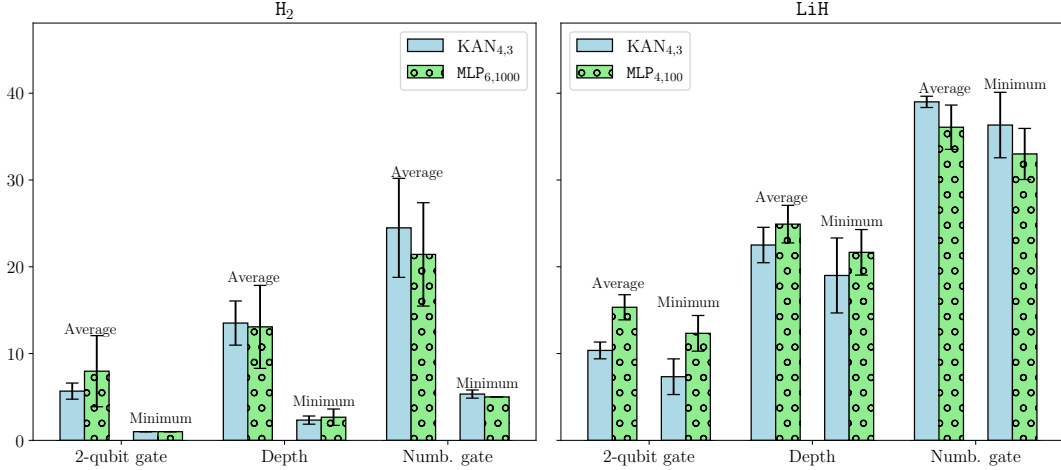


Fig. 4: KAN outperforms MLP in finding a parameterized quantum circuit that solves the 4-qubit LiH and H₂ molecule. We solve a molecule when its energy goes below the chemical accuracy, i.e., 1.6×10^{-3} Hartree. In the plot, the average corresponds to the average performance of the neural networks over three distinct initializations, and the minimum is the best-performing seed among the three. We consider KAN_{4,3} that corresponds to a KAN of depth 4 and 3 neurons, whereas MLP_{6,1000} and MLP_{4,100} defines MLP of depth 6 with 1000 neurons and MLP of depth 4 with 100 neurons respectively. It should be noted that an MLP of configuration MLP_{6,1000} outperforms KAN in the number of 2-qubit gates, depth, and the total number of parameters, but the number of trainable parameters required for the MLP is 5.15×10^6 which is very large compared to 5.52×10^4 parameters of KAN.

Problem	Network	Configuration	Spline and grid	Parameter count
Bell state prep. (noiseless)	KAN	KAN _{2,2}	B-spline, $k = 3, G = 5$	1728
	MLP	MLP _{4,30}	NA	4782
GHZ state prep. (noiseless)	KAN	KAN _{2,3}	B-spline, $k = 3, G = 5$	5562
	MLP	MLP _{4,30}	NA	11181
Bell state prep. (noisy)	KAN	KAN _{3,10}	B-spline, $k = 4, G = 5$	9540
	MLP	MLP _{4,100}	NA	29912
H ₂ ground state	KAN	KAN _{4,3}	B-spline, $k = 4, G = 5$	5.525×10^4
	MLP	MLP _{6,1000}	NA	5.150×10^6
LiH ground state	KAN	KAN _{4,3}	B-spline, $k = 4, G = 5$	5.525×10^4
	MLP	MLP _{4,100}	NA	1.348×10^5

TABLE III: KAN requires 2-3 \times less learnable parameters in the task of quantum state preparation. Meanwhile, in finding the ground state of LiH and H₂ KAN takes 2.4-93 \times fewer parameters respectively and still solves the problems with smaller parameterized quantum circuits than MLP. To simplify, we denote the networks by their depth and number of neurons. For instance, a KAN with configuration [288, 3, 21] is abbreviated as KAN_{2,3}, where 2 represents the network depth (excluding the input layer) and 3 denotes the number of neurons in the hidden layer. The same shorthand notation is applied to MLP networks.

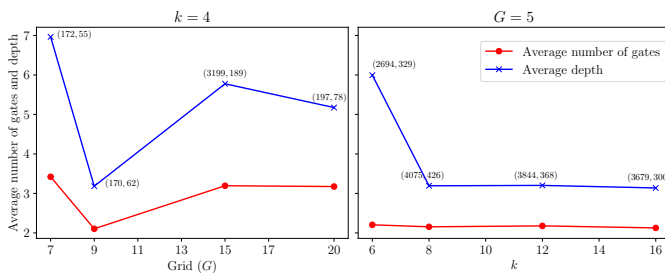


Fig. 5: The number of splines (k) has more impact in improving and stabilizing the performance of the KAN than the grid size (G). Here we measure the improvement of the KAN while constructing the GHZ state by calculating the average number of gates and depth in each setting. Each point is marked as (a, b) where a is the total number of successful episodes and b total optimal successful episodes.

is 120 \times higher. A recently released version of KAN, named MultKAN [39], executes an episode approximately 3.46 \times slower than MLPs.

VI. DISCUSSION AND FUTURE WORK

In this work, we analyse the practicality of using the recently introduced Kolmogorov-Arnold Networks in constructing quantum circuits in terms of probability of success, frequency of optimal solutions and the degrees of freedom of the network. To this end, we propose KANQAS which replaces the Multi-Layer Perception (MLP) in reinforcement learning-assisted quantum architecture search in the double deep Q-network with the Kolmogorov Arnold network (KAN).

Our experiments with KANQAS reveal that in constructing multi-qubit maximally entangled states with non-

Problem	Network	Configuration	Avg. time per episode
GHZ state prep.	KAN	KAN _{2,3}	0.2049
	MLP	MLP _{4,30}	0.0592
H ₂ ground state	KAN	KAN _{4,3}	2.2103
	MLP	MLP _{6,1000}	0.7552
LiH ground state	KAN	KAN _{4,3}	3.3737
	MLP	MLP _{4,100}	1.2102

TABLE IV: A new version of KAN [39] is approximately $3.46\times$ slower than MLPs, which is far better than the older version, which was $120\times$ slower for quantum state preparation. Meanwhile, KAN is $2.92\times$ and $2.787\times$ slower than MLP in finding the ground state of 4-qubit H₂ and LiH molecule respectively.

parameterized gates KAN can increase the probability of success of the RL agent in finding optimal quantum circuits as compared to MLPs. Moreover, when noise is present in the quantum device, achieving similar or better outcomes with an MLP necessitates a deeper and wider network compared to KAN, as well as a careful selection of the appropriate activation function. Since finding the optimal activation function for deep learning remains an ongoing challenge [40], [41], KAN has an advantage, as its activation functions are inherently learnable.

In addressing quantum chemistry problems, KAN demonstrates the ability to provide a more compact parameterized quantum circuit, with less number of 2 qubit gate and depth for finding the ground state of the chemical Hamiltonian using VQE, with a significantly reduced number of learnable parameters. It is important to note that for larger configurations, such as MLP_{6,1000}, MLP outperforms KAN configurations but requires 5-100 \times more learnable parameters. When considering a comparable number of learnable parameters, for example, MLP_{4,500} and KAN_{4,50}, KAN achieves the ground state with a parameterized quantum circuit of smaller depth and fewer 2-qubit gates. Although MLP results in a lower error in estimating the ground state, our objective in quantum chemistry is to attain chemical accuracy, defined as 1.6×10^{-3} Hartree. Given that the noise in 2-qubit gates is significantly higher than in 1-qubit gates [38], KAN demonstrates considerable promise for solving quantum chemistry problems on real quantum hardware.

Although the number of learnable parameters in KAN is on average 2-100 \times lesser than in MLPs, one of the biggest disadvantages of KAN is that it requires 2-3 \times more execution time per episode as compared to MLPs. However, due to their effectiveness and efficiency in finding solutions in noiseless and noisy quantum devices, KAN thus appears to be a reasonable alternative to traditional MLPs in solving quantum architecture search problems. In the following, we discuss the future research directions as a follow-up to our research.

- **KAN for VQAs** A primary direction for future research is addressing the quantum architecture search problem within variational quantum algorithms, in this paper we just show the simulation of 4-qubit H₂ and LiH molecules, this study should be expanded to bigger molecules such as H₂O 8-qubits. These KAN-assisted algorithms could have significant applications in quantum chemistry and combinatorial optimization problems.
- **Optimizing computational time of KAN** Another important goal is to explore the use of specialized accel-

erators, such as tensor processing units or digital signal processors, to reduce the computation time of KAN.

- **Interpretability of KAN** Focusing on the interpretability of KAN, future research should investigate its applicability to similar but scalable problems to enhance understanding. This can, for example, include the investigation of subclasses of families of the activation function after training KAN. We invite readers to explore our Git repository [42] for inspiration and further motivation in this direction.

VII. ACKNOWLEDGEMENT

AK would like to thank Ziming Liu for fruitful discussions about KAN. AK wish to thank the Finnish Computing Competence Infrastructure (FCCI) for supporting this project with computational and data storage resources.

APPENDIX

A. Double Deep Q-Network (DDQN)

Deep Reinforcement Learning (RL) techniques utilize Neural Networks (NNs) to adapt the agent’s policy to optimize the return:

$$G_t = \sum_{k=0}^{\infty} \gamma^k r_{t+k+1}, \quad (13)$$

where $\gamma \in [0, 1)$ is the discount factor. For each state-action pair (s, a) , an action value is assigned, quantifying the expected return from state s at step t when taking action a under policy π :

$$q_{\pi}(s, a) = \mathbb{E}_{\pi}[G_t | s_t = s, a_t = a]. \quad (14)$$

The goal is to determine the optimal policy that maximizes the expected return, which can be derived from the optimal action-value function q_* , defined by the Bellman optimality equation:

$$q_*(s, a) = \mathbb{E} \left[r_{t+1} + \max_{a'} q_*(s_{t+1}, a') | s_t = s, a_t = a \right]. \quad (15)$$

Instead of solving the Bellman optimality equation directly, value-based RL aims to learn the optimal action-value function from data samples. Q-learning is a prominent value-based RL algorithm, where each state-action pair (s, a) is assigned a Q-value $Q(s, a)$, which is updated to approximate q_* . Starting

from randomly initialized values, the Q-values are updated according to the rule:

$$Q(s_t, a_t) \leftarrow Q(s_t, a_t) + \alpha \left(r_{t+1} + \gamma \max_{a'} Q(s_{t+1}, a') - Q(s_t, a_t) \right), \quad (16)$$

where α is the learning rate, r_{t+1} is the reward at time $t + 1$, and s_{t+1} is the state encountered after taking action a_t in state s_t . This update rule is proven to converge to the optimal Q-values in the tabular case if all (s, a) pairs are visited infinitely often [43]. To ensure sufficient exploration in a Q-learning setting, an ϵ -greedy policy is used. Formally, the policy is defined as:

$$\pi(a|s) := \begin{cases} 1 - \epsilon_t & \text{if } a = \max_{a'} Q(s, a'), \\ \epsilon_t & \text{otherwise.} \end{cases} \quad (17)$$

The ϵ -greedy policy introduces randomness to the actions during training, but after training, a deterministic policy is used.

We employ NN ad function approximations to extend Q-learning to large state and action spaces. NN training typically requires independently and identically distributed data. This problem is circumvented by experience replay. This method divides experiences into single-episode updates and creates batches which are randomly sampled from memory. For stabilizing training, two NNs are used: a policy network, which is continuously updated, and a target network, which is an earlier copy of the policy network. The current value is estimated by the policy network, while the target network provides a more stable target value Y given by :

$$Y_{\text{DQN}} = r_{t+1} + \gamma \max_{a'} Q_{\text{target}}(s_{t+1}, a'). \quad (18)$$

In the DDQN algorithm, we sample the action for the target value from the policy network to reduce the overestimation bias present in standard DQN. The corresponding target is defined as:

$$Y_{\text{DDQN}} = r_{t+1} + \gamma Q_{\text{target}} \left(s_{t+1}, \arg \max_{a'} Q_{\text{policy}}(s_{t+1}, a') \right). \quad (19)$$

This target value is approximated via a loss function. In this work, we consider the loss function as the smooth L1-norm.

B. Configuration of neural networks

The detailed configurations of the KANs and the MLPs utilized in the main text to tackle quantum state preparation and quantum chemistry problems are provided in Tab. V and Tab. VI

C. Quantum chemistry with different configurations of KAN and MLP

In this section, we further explore the different configurations of KAN and MLP in finding the ground state of the 4-qubit `LiH` molecule. We use the following variables to benchmark the performance of the different neural networks: the minimum number of 1-qubit gates (Min. 1-qubit gate), the minimum number of 2-qubit gates (Min 2-qubit gate), the error in estimating the ground state energy (error), and the number of learnable parameters in the network (Parameter count). The results are presented in detail in the Tab. VII.

From the Tab. VII we observe although the `MLP6,1000` provides us with the best result in terms of all the benchmarking variables, the number of learnable parameters it requires to achieve this outcome is $10\times$ higher than `KAN4,30`, which is far more expensive in terms of training time. Meanwhile, for the sake of fair comparison, if we observe the performance of `KAN4,50` and `MLP4,500` where the number of parameters in MLP is $1.078\times$ more than KAN, we notice a tradeoff between the number of parameterized 1-qubit gates and the number of 2-qubit gates. The KAN provides us with a competitive approximation of the ground state with a shorter parameterized quantum circuit, containing less 2-qubit gate and smaller depth than MLP despite having a smaller number of parameters. Considering that the noise in 2-qubit gates in real quantum hardware is many scales higher than 1-qubit gates, KAN with a comparable number of parameters, shows a large potential in quantum architecture search in quantum hardware.

Network	Problem	Configuration	Spline and grid	Activation func.
KAN	Bell state prep.	KAN _{2,2}	B-spline, $k = 3, G = 5$	learnable
	GHZ state prep.	KAN _{2,3}	B-spline, $k = 4, G = 5$	learnable
MLP	Bell state prep.	MLP _{4,30}	NA	LeakyReLU
	GHZ state prep.	KAN _{2,3}		
	GHZ state prep.	KAN _{4,30}		

TABLE V: Configuration for noiseless GHZ and Bell state preparation. In the case of MLP, the activation function is fixed whereas it is learned during the network training for KAN. For the sake of simplicity, we represent the networks by their depth and number of neurons for example, for a KAN of configuration [288, 3, 21], we use the shorthand notation KAN_{2,3} as the KAN is of depth 2 (excluding the input layer) and contains 3 neurons in the hidden layer.

Network	Molecule	Network configuration	Spline and grid	Activation func.
KAN	H ₂	KAN _{4,3}	B-spline, $k = 10, G = 5$	learnable
	LiH	KAN _{2,3}		
		KAN _{4,30} KAN _{4,50}		
MLP	H ₂	MLP _{6,1000}	NA	LeakyReLU
	LiH	MLP _{4,100}		
		MLP _{4,500} MLP _{6,1000}		

TABLE VI: The configuration of KAN and MLP utilized in tackling quantum chemistry problems specifically for finding the ground state of 4-qubit H₂ and LiH molecule. A detailed configuration of these molecules is in Tab. I. As discussed in the caption of Tab. V, we represent the networks by their depth and number of neurons for example, for an MLP of configuration [1121, 500, 500, 500, 24], we use the shorthand notation MLP_{4,500} as the MLP of depth 4 (excluding the input layer) and of 500 neurons in the hidden layer.

Molecule	Network configuration	Min. 2-qubit gate	Min. depth	Min. 1-qubit gate	error	Parameter count
4-qubit	KAN _{4,30}	11	18	15	1.129×10^{-4}	5.784×10^5
	KAN _{4,50}	8	17	24	2.265×10^{-4}	9.960×10^5
LiH	MLP _{4,500}	13	18	13	1.100×10^{-4}	1.074×10^6
	MLP _{6,1000}	6	11	13	3.606×10^{-5}	5.152×10^6

TABLE VII: We observe that although MLP_{6,1000} gives the best results in all benchmarking variables, it requires $10\times$ more learnable parameters than KAN_{4,30}, making it significantly more expensive in terms of training time. For a fair comparison, KAN_{4,50} and MLP_{4,500} show a tradeoff between the number of parameterized 1-qubit gates and 2-qubit gates, with MLP_{4,500} having 1.078 times more parameters than KAN_{4,50}. Despite having fewer parameters, KAN provides a competitive approximation of the ground state with a shorter parameterized quantum circuit, fewer 2-qubit gates, and smaller depth than MLP.

REFERENCES

- [1] P. Ren, Y. Xiao, X. Chang, P.-Y. Huang, Z. Li, X. Chen, and X. Wang, "A comprehensive survey of neural architecture search: Challenges and solutions," *ACM Computing Surveys (CSUR)*, vol. 54, no. 4, pp. 1–34, 2021.
- [2] S.-X. Zhang, C.-Y. Hsieh, S. Zhang, and H. Yao, "Differentiable quantum architecture search," *Quantum Science and Technology*, vol. 7, no. 4, p. 045023, 2022.
- [3] Z. Lu, P.-X. Shen, and D.-L. Deng, "Markovian quantum neuroevolution for machine learning," *Physical Review Applied*, vol. 16, no. 4, p. 044039, 2021.
- [4] J. R. McClean, J. Romero, R. Babbush, and A. Aspuru-Guzik, "The theory of variational hybrid quantum-classical algorithms," *New Journal of Physics*, vol. 18, no. 2, p. 023023, 2016.
- [5] M. Cerezo, A. Arrasmith, R. Babbush, S. C. Benjamin, S. Endo, K. Fujii, J. R. McClean, K. Mitarai, X. Yuan, L. Cincio *et al.*, "Variational quantum algorithms," *Nature Reviews Physics*, vol. 3, no. 9, pp. 625–644, 2021.
- [6] A. Sarkar, "Automated quantum software engineering," *Automated Software Engineering*, vol. 31, no. 1, pp. 1–17, 2024.
- [7] E.-J. Kuo, Y.-L. L. Fang, and S. Y.-C. Chen, "Quantum architecture search via deep reinforcement learning," *arXiv preprint arXiv:2104.07715*, 2021.
- [8] M. Ostaszewski, L. M. Trenkwalder, W. Masarczyk, E. Scerri, and V. Dunjko, "Reinforcement learning for optimization of variational quantum circuit architectures," *Advances in Neural Information Processing Systems*, vol. 34, pp. 18 182–18 194, 2021.
- [9] A. Kundu, P. Bedelek, M. Ostaszewski, O. Danaci, Y. J. Patel, V. Dunjko, and J. A. Mischak, "Enhancing variational quantum state diagonalization using reinforcement learning techniques," *New Journal of Physics*, vol. 26, no. 1, p. 013034, 2024.
- [10] Y. Du, T. Huang, S. You, M.-H. Hsieh, and D. Tao, "Quantum circuit architecture search for variational quantum algorithms," *npj Quantum Information*, vol. 8, no. 1, p. 62, 2022.
- [11] Y. J. Patel, A. Kundu, M. Ostaszewski, X. Bonet-Monroig, V. Dunjko, and O. Danaci, "Curriculum reinforcement learning for quantum architecture search under hardware errors," *arXiv preprint arXiv:2402.03500*, 2024.
- [12] A. Sadhu, A. Sarkar, and A. Kundu, "A quantum information theoretic analysis of reinforcement learning-assisted quantum architecture search," *arXiv preprint arXiv:2404.06174*, 2024.
- [13] A. R. Morgillo, S. Mangini, M. Piastra, and C. Macchiavello, "Quantum state reconstruction in a noisy environment via deep learning," *Quantum Machine Intelligence*, vol. 6, no. 2, 2024. [Online]. Available: <http://dx.doi.org/10.1007/s42484-024-00168-x>
- [14] A. Lumino, E. Polino, A. S. Rab, G. Milani, N. Spagnolo, N. Wiebe, and F. Sciarrino, "Experimental phase estimation enhanced by machine learning," *Physical Review Applied*, vol. 10, no. 4, p. 044033, 2018.
- [15] S. Wang, E. Fontana, M. Cerezo, K. Sharma, A. Sone, L. Cincio, and P. J. Coles, "Noise-induced barren plateaus in variational quantum algorithms," *Nature Communications*, vol. 12, no. 1, p. 6961, 2021.
- [16] L. Bittel and M. Kliesch, "Training variational quantum algorithms is np-hard," *Physical Review Letters*, vol. 127, p. 120502, Sep 2021. [Online]. Available: <https://link.aps.org/doi/10.1103/PhysRevLett.127.120502>
- [17] Z. Liu, Y. Wang, S. Vaidya, F. Ruehle, J. Halverson, M. Soljačić, T. Y. Hou, and M. Tegmark, "Kan: Kolmogorov-arnold networks," *arXiv preprint arXiv:2404.19756*, 2024.
- [18] A. A. Aghaei, "fkan: Fractional kolmogorov-arnold networks with trainable jacobi basis functions," *arXiv preprint arXiv:2406.07456*, 2024.
- [19] R. Genet and H. Inzirillo, "Tkan: Temporal kolmogorov-arnold networks," *arXiv preprint arXiv:2405.07344*, 2024.
- [20] Z. Bozorgasl and H. Chen, "Wav-kan: Wavelet kolmogorov-arnold networks," *arXiv preprint arXiv:2405.12832*, 2024.
- [21] D. W. Abueidda, P. Pantidis, and M. E. Mobasher, "Deepokan: Deep operator network based on kolmogorov arnold networks for mechanics problems," *arXiv preprint arXiv:2405.19143*, 2024.
- [22] M. Kiamari, M. Kiamari, and B. Krishnamachari, "Gkan: Graph kolmogorov-arnold networks," *arXiv preprint arXiv:2406.06470*, 2024.
- [23] J. Xu, Z. Chen, J. Li, S. Yang, W. Wang, X. Hu, and E. C.-H. Ngai, "Fourierkan-gcf: Fourier kolmogorov-arnold network—an effective and efficient feature transformation for graph collaborative filtering," *arXiv preprint arXiv:2406.01034*, 2024.
- [24] R. Genet and H. Inzirillo, "A temporal kolmogorov-arnold transformer for time series forecasting," *arXiv preprint arXiv:2406.02486*, 2024.
- [25] K. Xu, L. Chen, and S. Wang, "Kolmogorov-arnold networks for time series: Bridging predictive power and interpretability," *arXiv preprint arXiv:2406.02496*, 2024.
- [26] C. J. Vaca-Rubio, L. Blanco, R. Pereira, and M. Caus, "Kolmogorov-arnold networks (kans) for time series analysis," *arXiv preprint arXiv:2405.08790*, 2024.
- [27] M. Cheon, "Kolmogorov-arnold network for satellite image classification in remote sensing," *arXiv preprint arXiv:2406.00600*, 2024.
- [28] Y. Wang, J. Sun, J. Bai, C. Anitescu, M. S. Eshaghi, X. Zhuang, T. Rabczuk, and Y. Liu, "Kolmogorov arnold informed neural network: A physics-informed deep learning framework for solving pdes based on kolmogorov arnold networks," *arXiv preprint arXiv:2406.11045*, 2024.
- [29] I. N. Levine, D. H. Busch, and H. Shull, *Quantum chemistry*. Pearson Prentice Hall Upper Saddle River, NJ, 2009, vol. 6.
- [30] A. N. Kolmogorov, "On the representation of continuous functions of many variables by superposition of continuous functions of one variable and addition," in *Doklady Akademii Nauk*, vol. 114, no. 5. Russian Academy of Sciences, 1957, pp. 953–956.
- [31] K. Hornik, M. Stinchcombe, and H. White, "Multilayer feedforward networks are universal approximators," *Neural networks*, vol. 2, no. 5, pp. 359–366, 1989.
- [32] G. D. Knott, *Interpolating cubic splines*. Springer Science & Business Media, 1999, vol. 18.
- [33] D. E. Rumelhart, R. Durbin, R. Golden, and Y. Chauvin, "Backpropagation: The basic theory," in *Backpropagation*. Psychology Press, 2013, pp. 1–34.
- [34] R. Waris and Corentin, "Kolmogorov-Arnold Q-Network (KAQN)-KAN applied to Reinforcement learning, initial experiments," <https://github.com/rriiswa/kanrl>, 2024.
- [35] H. Van Hasselt, A. Guez, and D. Silver, "Deep reinforcement learning with double q-learning," in *Proceedings of the AAAI conference on artificial intelligence*, vol. 30, no. 1, 2016.
- [36] V. Mnih, K. Kavukcuoglu, D. Silver, A. A. Rusu, J. Veness, M. G. Bellemare, A. Graves, M. Riedmiller, A. K. Fidjeland, G. Ostrovski *et al.*, "Human-level control through deep reinforcement learning," *nature*, vol. 518, no. 7540, pp. 529–533, 2015.
- [37] Y. Chen, L. Zhang, H. Wang, and W. E, "Ground state energy functional with hartree-fock efficiency and chemical accuracy," *The Journal of Physical Chemistry A*, vol. 124, no. 35, pp. 7155–7165, 2020.
- [38] E. Wilson, F. Mueller, L. Bassman Otfelie, and C. Iancu, "Empirical evaluation of circuit approximations on noisy quantum devices," in *Proceedings of the International Conference for High Performance Computing, Networking, Storage and Analysis*, 2021, pp. 1–15.
- [39] "MultKAN," <https://github.com/KindXiaoming/pykan/blob/master/kan/MultKAN.py>, 2024.
- [40] S. Hayou, A. Doucet, and J. Rousseau, "On the selection of initialization and activation function for deep neural networks," *arXiv preprint arXiv:1805.08266*, 2018.
- [41] P. Ramachandran, B. Zoph, and Q. V. Le, "Searching for activation functions," *arXiv preprint arXiv:1710.05941*, 2017.
- [42] A. Kundu, "KANQAS GitHub," https://github.com/Aqasch/KANQAS_code, 2024.
- [43] F. S. Melo, "Convergence of q-learning: A simple proof," *Institute Of Systems and Robotics, Tech. Rep.*, pp. 1–4, 2001.